Journal of the Korean Astronomical Society
54: 129 ∼ 137, 2021 August
https://doi.org/10.5303/JKAS.2021.54.4.129
pISSN: 1225-4614 · eISSN: 2288-890X
http://jkas.kas.org

Temporal Variations of the Global Seismic Parameters of HD 49933 over a Magnetic Cycle

Ki-Beom Kim and Heon-Young Chang

Department of Astronomy and Atmospheric Sciences, Kyungpook National University, Daegu 41566, Korea; hyc@knu.ac.kr

Received May 7, 2021; accepted July 1, 2021

Abstract: It has been established that the acoustic mode parameters of the Sun and Sun-like stars vary over activity cycles. Since the observed variations are not consistent with an activity-related origin, even Sun-like stars showing out-of-phase changes of mode frequencies and amplitudes need to be carefully studied using other observational quantities. In order to test whether the presumed relations between the global seismic parameters are a signature of the stellar activity cycle, we analyze the photometric light curve of HD 49933 for which the first direct detection of an asteroseismic signature for activity-induced variations in a Sun-like star was made, using observations by the CoRoT space telescope. We find that the amplitude of the envelope significantly anti-correlates with both the maximum frequency of the envelope and the width of the envelope unless superflare-like events completely contaminate the light curve. However, even though the photometric proxy for stellar magnetic activity appears to show relations with the global asteroseismic parameters, they are statistically insignificant. Therefore, we conclude that the global asteroseismic parameters can be utilized in cross-checking asteroseismic detections of activity-related variations in Sun-like stars, and that it is probably less secure and effective to construct a photometric magnetic activity proxy to indirectly correlate the global asteroseismic parameters. Finally, we seismically estimate the mass of HD 49933 based on our determination of the large separation of HD 49933 with evolutionary tracks computed by the MESA code and find a value of about $1.2 M_{\odot}$ and a sub-solar metallicity of $Z = 0.008$, which agrees with the current consensus and with asteroseismic and non-asteroseismic data.

Key words: asteroseismology — stars: magnetic field — methods: data analysis — stars: individual: HD 49933

1. Introduction

Turbulent flows in the convective envelopes of the Sun and Sun-like stars, which is inevitably affected by the stellar magnetism, generate resonant sound waves trapped in the stellar interiors and are observed as non-radial oscillations (Goldreich & Keeley 1977; Goldreich & Kumar 1988; Goldreich et al. 1994; Balmforth 1992). Exploring the observed individual mode frequencies of the oscillations allows us to improve our knowledge on the internal structure and dynamics of the Sun and other stars (Christensen-Dalsgaard et al. 1985; Gough 1985, 1990; Elsworth et al. 1995; Thompson et al. 1996; Basu et al. 1997; Christensen-Dalsgaard 2002; Aerts et al. 2010; Appourchaux et al. 2010). Furthermore, it has been established that solar acoustic mode parameters change with the solar activity level (Woodard & Noyes 1985; Fossat et al. 1987; Pallé et al. 1989; Elsworth et al. 1990, 1994; Libbrecht & Woodard 1990; Chaplin et al. 1998, 2001, 2004). The amplitude (frequency and damping rate) of the acoustic mode is (are) observed to decrease (increase) with increasing solar magnetic activity (Elsworth et al. 1993; Chaplin et al. 2000; Komm et al. 2000). Modulations with the solar activity cycle can be understood by considering that the background magnetic field suppresses the turbulent convection and subsequently the excitation of sound waves, causing changes in the boundary conditions of the acoustic cavity in which they propagate (Jiménez-Reyes et al. 2003). Helioseismology has thus provided important inputs for dynamo theories by measuring such activity-related variations.

It is natural to expect from asteroseismic observations of Sun-like stars that the observed parameters of the individual acoustic modes vary as the stellar magnetic cycle continues, following a similar trend to that observed in the Sun. If this is indeed the case, it would be worthwhile to accumulate observational data of activity-related variations over several magnetic cycles in active stars other than the Sun; our knowledge of dynamo processes can be greatly improved by providing observational constraints for stellar dynamo models for different evolutionary stages and under physical conditions distinct from those of the Sun (e.g., Chaplin et al. 2007; Metcalfe et al. 2007; Thomas et al. 2021). In addition to monitoring long-term chromospheric Ca II H&K emission (Baliunas et al. 1995; Henry et al. 1996; Radick et al. 1998; Ak et al. 2001; Isaacson & Fischer 2010; Meunier et al. 2019), the first direct detection of an asteroseismic signature of activity-induced variations in a Sun-like star was achieved for HD 49933 (also

Corresponding author: H.-Y. Chang

known as HR 2530 and CoRoT 20), an F5V star ∼20% more massive and ∼34% larger than the Sun with a surface rotation period of 3.5 days (García et al. 2010; Salabert et al. 2011; Régulo et al. 2016). García et al. (2010) reported anti-correlated temporal variations of the mode amplitude and frequency, as observed for the Sun. Moreover, the observed frequency shifts show a clear dependence on the mode frequency, reaching a maximum shift of ∼2 μHz around 2100 μHz (Salabert et al. 2011), which is ascribed to changes in the near-surface layers due to the local magnetic activity.

It should be kept in mind, however, that a subsequent study that measured temporal variations in frequency shifts for 87 Sun-like stars shows that the mode frequencies and amplitudes of at least ∼20% of the diagnosed stars change in phase instead of out of phase, i.e., in opposition to what is seen for the Sun (Santos et al. 2018, 2019). This implies that not all of the observed variability may be associated with the stellar magnetism. For example, the unexpected relation between the mode amplitude and frequency shift could arise due to stochastic fluctuations during minima of the stellar activity cycle. Hence, even Sun-like stars showing the out-of-phase change of mode frequencies and amplitudes need to be confirmed with due care.

In *ensemble asteroseismology*, fundamental stellar quantities, such as mass and radius, are inferred from parameters describing the Gaussian envelope of the stellar oscillation power excess (Brown & Gilliland 1994; Kjeldsen & Bedding 1995, 2011; Belkacem et al. 2011, 2013; Chaplin & Miglio 2013; Hekker 2020). Asteroseismic scaling relations have provided evidence that the global asteroseismic parameters are functions of stellar parameters such as evolutionary status, rotational period, age, effective temperature, metallicity, and magnetic activity. For example, magnetically active stars are apt to have a lower envelope amplitude for the stellar oscillation power excess of the pressure mode (p-mode) than less active stars (Mosser et al. 2009; Dall et al. 2010; Chaplin et al. 2011; Huber et al. 2011; Kim & Chang 2021a). For the frequency of the maximum height in the acoustic power spectrum, $\nu_{\rm max}$, a positive correlation is expected with stellar activity, provided that the stellar acoustic cutoff frequency correlating with stellar activity is proportional to $\nu_{\rm max}$ (Jiménez et al. 2011; Howe et al. 2020). One may also expect a positive correlation between the envelope width and stellar activity due to a synergy of (1) the differential suppression of mode amplitudes over wide frequency ranges (e.g., Salabert et al. 2003; Kjeldsen et al. 2008) and (2) the proportional increase of frequency shift by an activity-related origin in the mode frequency (e.g., Gelly et al. 2002; Howe et al. 2002). As a result of these two, the envelope of the acoustic oscillation becomes flatter and broader as solar activity proceeds to its maximum.

In order to uncover signatures of the stellar activity cycle in the light curve of Sun-like stars, we probe the behavior of the relations among the global seismic parameters. For this purpose, we analyze photometric data of HD 49933 observed by the COnvection, ROtation and planetary Transits (CoRoT) space telescope, led by the French Space Agency in conjunction with the European Space Agency, as a case study. In the course of investigation, we also asteroseismically constrain the mass of HD 49933 by comparing theoretical evolution models constructed from the MESA code with the observed location in the seismic Hertzsprung-Russell diagram. This paper is organized as follows. We begin with a description of the data analyzed in the current paper and methods used to acquire envelope parameters for the stellar oscillation power excess in Section 2. We present the relations deduced from temporal variations of the global seismic parameters in Section 3. We place HD 49933 in the seismic H–R diagram and briefly discuss its implication on mass estimation in Section 4. Finally, we summarize the results and conclude the study in Section 5.

Table 1
Stellar parameters of HD 49933

Parameter	Unit	HD 49933	Reference
Spec. type	—	F5V	Mosser et al. (2005)
m_v	mag	5.866±0.001	van Leeuwen (2007)
$B-V$	mag	0.396±0.007	van Leeuwen (2007)
π	mas	33.45±0.84	van Leeuwen (2007)
[Fe/H]	dex	−0.29	Cenarro et al. (2007)
$T_{\rm eff}$	K	6590±60	Bruntt (2009)
log g	cgs	4.21±0.14	Bigot et al. (2011)
$L_\star$	$L_\odot$	3.47±0.18	Bruntt (2009)
$M_\star$	$M_\odot$	1.19±0.07	Benomar et al. (2010)
$R_\star$	$R_\odot$	1.385±0.031	Bruntt (2009)
Age	Gyr	2.15	Kallinger et al. (2010)
$v_{\rm rot}\sin i$	km s^{-1}	−12.8±0.3	Gontcharov (2006)

2. DATA

For the seismic analysis of Sun-like oscillations in the star HD 49933, we extracted the CoRoT level-N2 light curve with a cadence of 32 seconds, corresponding to a Nyquist frequency of ∼ 15000 μHz, which is available in the Instituto de Astrofisica de Canarias (IAC) CoRoT Public Archive[1] (Chaintreuil et al. 2016). HD 49933 has been observed three times, for 60 days in 2007, 137 days in 2008, and 60 days in 2012 (Appourchaux et al. 2008; Benomar et al. 2009). The CoRoT satellite operated from 2006 to 2013 and observed more than 160,000 stars in 26 stellar fields with a field of view of 3.05° × 2.7° without Earth occultations, allowing up to 150 days of continuous observation (Baglin et al. 2006; Michel et al. 2008). After the unfortunate failure of Data Processing Unit No. 1 in 2009, however, observations were limited to 3-month observing runs. Data sets are grouped into four levels, N0, N1, N2, and N3, based on the reduction processes. For example, invalid data are corrected with the *inpainting method* at level N2 (Pires et al. 2015).

In Figure 1, we show the light curves of HD 49933 from three separate observing runs by CoRoT, in which

[1] http://idoc-corot.ias.u-psud.fr

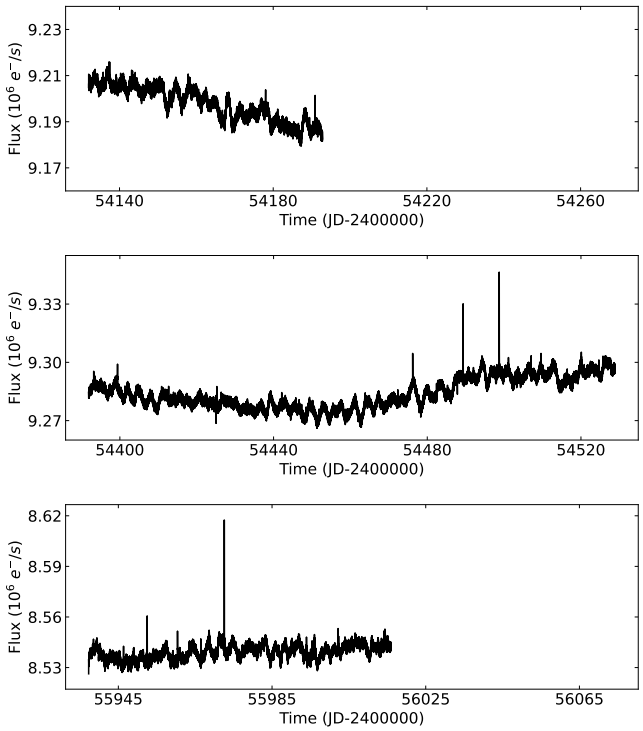

Figure 1. Light curves of HD 49933 observed by CoRoT for three separate observing runs, which are recorded with a cadence of 32 seconds for 60 days in 2007, 137 days in 2008, and 60 days in 2012 (from top to bottom, respectively). Note two superflare-like peaks from JD 2454480 to JD 2454520 which are suspected to be comparable to the Halloween solar storms in late 2003.

a quasi-periodic modulation with a period of ~ 3.5 days can be seen on top of a slow variation with a period of at least 120 days which hints at the stellar activity cycle. We assume that the short-term variation is due to the rotation of HD 49933, $\sim$8 times faster than the Sun, with star-spots being distributed over the visible surface. It is useful to note that the periods of activity cycles are known to be approximately proportional to the stellar spin periods. Interestingly, active and inactive stars appear to follow two distinct paths in that relation (Saar & Brandenburg 1999; Böhm-Vitense 2007).

To derive the global seismic parameters for the stellar oscillation power excess as a function of time, we have first removed outliers in the time series which deviate by more than 3σ and then detrended the data with a third-order polynomial function spanning two days. We computed a power spectrum for each 40-day-long time series shifted in steps of 10 days with the Lomb-Scargle algorithm (Lomb 1976; Scargle 1982) and smoothed it with a Gaussian moving average with a width of 5 μHz. Using the power spectrum for HD 49933, we fit a model to the acoustic power spectrum over the frequency range $\nu \geq 200$ μHz to extract the global seismic parameters with the Levenberg-Marquardt least-squares method. In the current analysis, we have only taken the second

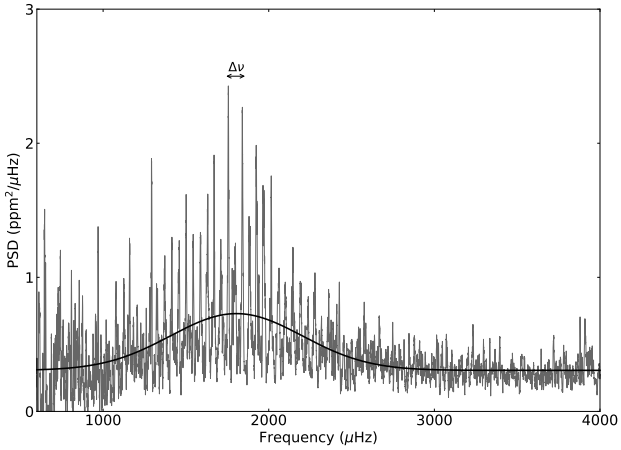

Figure 2. The power spectral density (PSD) of HD 49933 resulting from the first 40-day-long time series in the second observing run. Note that the PSD is shown after removing the background red noise with the Karoff model with $n = 2$. Thus, the thick curve represents the sum of the envelope profile of the power excess for the acoustic oscillation and the background white noise.

run of observations because it is the longest run and corresponds to the time series for which García et al. (2010) demonstrated anti-correlated variations in the mode frequency and amplitude of HD 49933, and because the light curves observed for the first and third runs show low signal-to-noise ratios.

The observed power spectrum, shown in Figure 2, is modeled with three standard components: the envelope profile of the power excess for the acoustic oscillation, $P(\nu)$, the background white shot noise, $W(\nu)$, and the background red noise representing various features in the solar atmosphere, $B(\nu)$. Even though some F-stars are reported to have a broad super-Gaussian shape (Appourchaux et al. 2008; Arentoft et al. 2008; Bedding et al. 2010), the envelope profile of the power excess is here given by the Gaussian profile

$$P(\nu) = A \exp\left[\frac{-(\nu_{\max} - \nu)^2}{2\sigma_e^2}\right], \qquad (1)$$

where $\nu_{\max}$ is the central frequency of the envelope profile for the stellar oscillation power excess, A is the height at $\nu_{\max}$, and $\delta\nu_{\rm env} = 2\sqrt{2\ln 2}\sigma_e$ is the full width at half maximum (FWHM) of the envelope profile. The background red noise is caused by various effects such as granulation, bright faculae, and chromospheric features. Considering that granulation and bright faculae dominate the background red-noise, we have employed a model of the background red noise of the stellar power spectrum proposed by Karoff (2008), the Karoff model with $n = 2$,

$$B(\nu) = \sum_{i=1}^{2} \left(\frac{4\sigma_i^2 \tau_i}{1 + (2\pi\nu\tau_i)^2 + (2\pi\nu\tau_i)^4}\right), \qquad (2)$$

where σ_i is the i-th component of the rms intensity and τ_i is the i-th characteristic time-scale of the rms

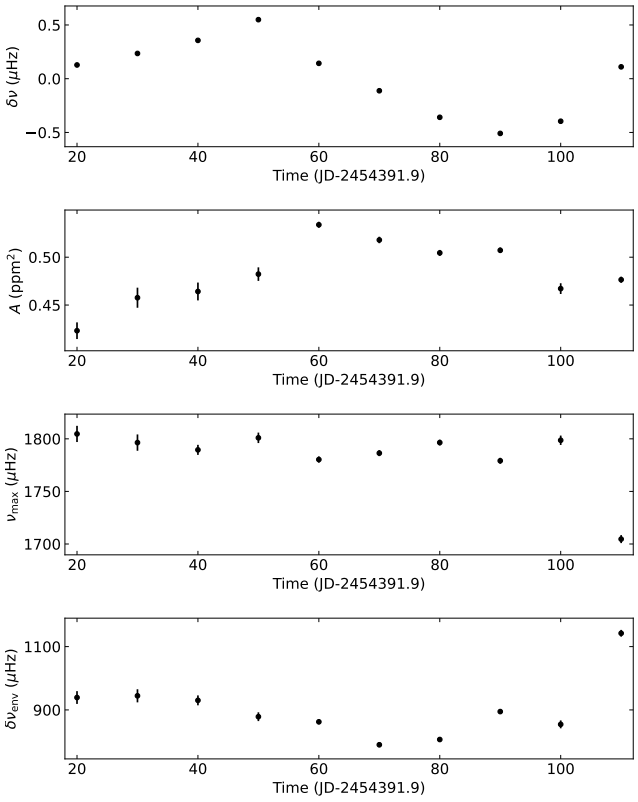

Figure 3. Temporal variations in $\delta\nu$, A, $\nu_{\rm max}$, and $\delta\nu_{\rm env}$ (from top to bottom, respectively). Data points result from each power spectrum of a 40-day-long time series shifted every 10 days in the second run of CoRoT observations.

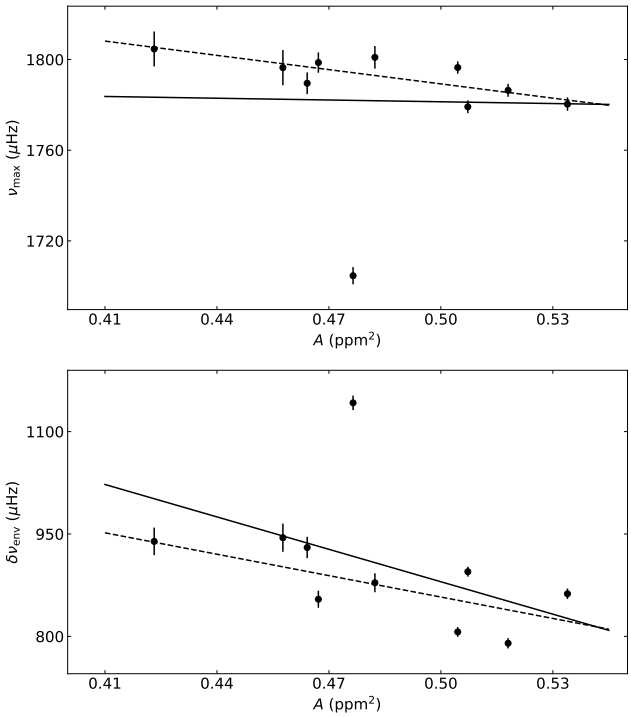

Figure 4. Scatter plots of $\nu_{\rm max}$ (top) and $\delta\nu_{\rm env}$ (bottom) against A. The solid and dashed lines represent the best fits resulting from 10 points and 9 points. See the text for details.

intensity, respectively. Note that we have marked the large separation in the acoustic power spectrum, $\Delta\nu$ in Figure 2. The large separation in the acoustic power spectrum is defined by the average frequency spacing between modes of adjacent radial order (n) for a given degree (l) and related to the mean density of a star (ρ) like $\Delta\nu \propto \sqrt{\bar{\rho}}$ (Tassoul 1980; Ulrich 1986; Christensen-Dalsgaard 1988).

3. GLOBAL SEISMIC PARAMETERS OF HD 49933

In Figure 3, we show temporal variations in the frequency shift of the acoustic mode, $\delta\nu$, the amplitude of the envelope, A, the central frequency of the envelope profile, $\nu_{\rm max}$, and the FWHM of the envelope profile, $\delta\nu_{\rm env}$, with error bars from top to bottom, respectively. To measure $\delta\nu$ as a function of time, instead of directly analyzing individual modes from the power spectrum and taking an average, we have calculated the cross-correlation between each power spectrum from a 40-day-long segment of the time series and the average of 10 power spectra obtained from 40-day-wide windows shifted by 10 days (Régulo et al. 2016). We have employed this approach here because the frequency resolution of the power spectrum of a 40-day-long time series is insufficient for the accurate analysis of individual modes. We emphasize that the frequency shift measured using cross-correlation methods is likely to be smoother than the frequency shift obtained from direct estimates by the analysis of individual modes, although the two different methods return consistent results (García et al. 2010; Santos et al. 2018). This is because dipole modes ($l = 1$) are weighted more than monopole modes ($l = 0$) by their intrinsic amplitudes in the cross-correlation techniques. As a result, correlation coefficients would be somewhat lower when a linear correlation coefficient with $\delta\nu$ measured using cross-correlation methods and other parameters are calculated. Already from visual inspection of the top two panels of Figure 3, it is evident that $\delta\nu$ in HD 49933 anti-correlates with A, as García et al. (2010) reported. We note that there is a time lag by ∼20–30 days while A appears to lead $\delta\nu$ by ∼15–20 days at most in García et al. (2010). Regarding the global seismic parameters shown in the bottom three panels, A, $\nu_{\rm max}$, and $\delta\nu_{\rm env}$, it appears that A anti-correlates with $\nu_{\rm max}$ and $\delta\nu_{\rm env}$ without a significant time lag.

To better examine the statistical behavior of the global asteroseismic parameters, we show scatter plots of $\nu_{\rm max}$ and $\delta\nu_{\rm env}$ against A in the upper and lower panels of Figure 4, respectively. We note that the acoustic power spectrum of HD 49933 seriously deteriorates due to two superflare-like peaks from JD 2454480 to JD 2454520 shown in Figure 1. The envelope of the solar oscillation power excess has abnormally low

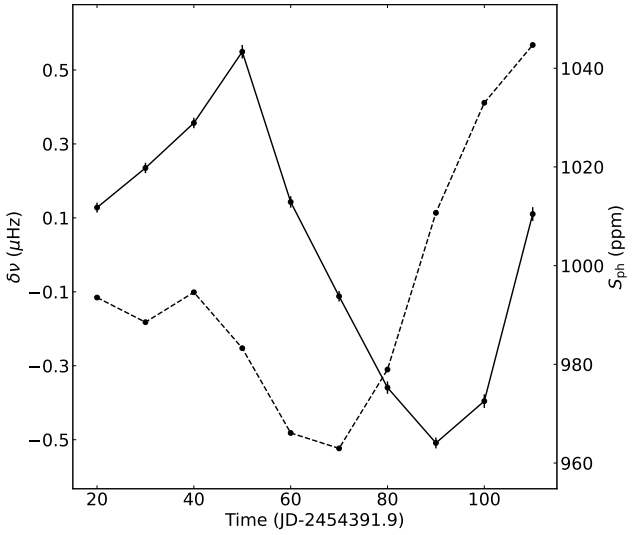

Figure 5. Frequency of the maximum height in the acoustic power spectrum, $\delta\nu$, together with the photometric proxy for stellar magnetic activity, $S_{\rm ph}$, as a function of time. The solid and dashed curves represent $\delta\nu$ and $S_{\rm ph}$, respectively.

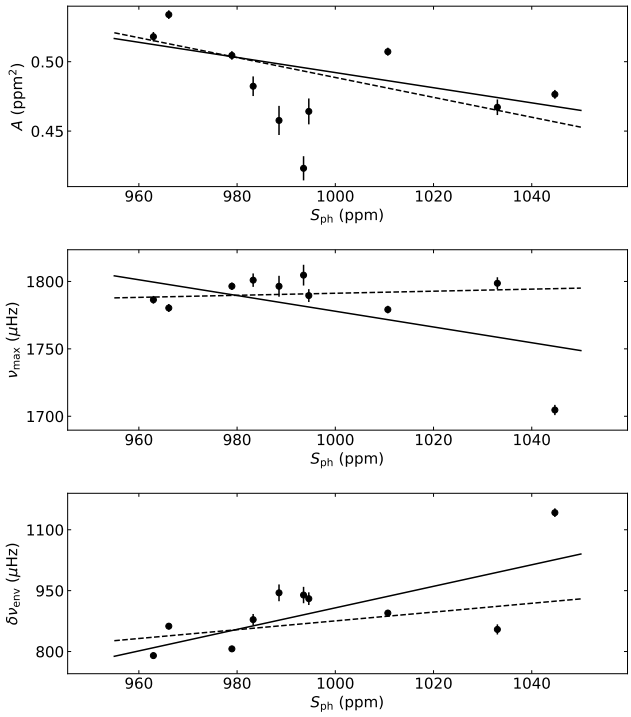

Figure 6. Scatter plots of A (top), $\nu_{\rm max}$ (center), and $\delta\nu_{\rm env}$ (bottom) against $S_{\rm ph}$. The solid and dashed lines represent the best fits resulting from 10 points and 9 points. See the text for details.

$\nu_{\rm max}$ and broad $\delta\nu_{\rm env}$ during that period. The events are suspected to be comparable to the Halloween solar storms that occurred from mid-October to early November 2003, peaking around October 28 and 29 in 2003, which were among the most powerful events in recent decades, estimated to be of class X45. We have noticed similar contamination in the parameter relations for the Halloween solar storms in the Solar case (Jo et al. 2021, in preparation). We have thus repeated calculating the best fit with 9 points instead of 10, omitting the data point we just mentioned. As a quantitative measure, we have calculated the Pearson linear correlation coefficient r and the corresponding false alarm probability P for A and $\nu_{\rm max}$ using 9 points and obtained $r = -0.7692$ with $P = 0.0154$. For A and $\delta\nu_{\rm env}$, the values are $r = -0.7069$ and $P = 0.0332$, respectively. The amplitude of the envelope significantly anti-correlates with both the maximum frequency of the envelope and the width of the envelope under ordinary circumstances. Therefore, we conclude that the global asteroseismic parameters can be utilized for cross-checking asteroseismic detections of activity-related variations in Sun-like stars.

In Figure 5, for a direct comparison of $\delta\nu$ with the magnetic activity of HD 49933, we show $\delta\nu$ with error bars, together with the photometric proxy for stellar magnetic activity, $S_{\rm ph}$, as a function of time. Since $S_{\rm ph}$ is widely used to search for magnetic-field related trends in asteroseismology, we have produced $S_{\rm ph}$ from our time series with the dispersion of the light curve measured on time scales of five times the rotation period (Mathur et al. 2014). It is interesting to note that $\delta\nu$ is correlated with $S_{\rm ph}$ while $S_{\rm ph}$ leads $\delta\nu$ by approximately 20 days. This apparent behavior agrees with the finding by García et al. (2010) that their starspot proxy is shifted ∼30–40 days relative to $\delta\nu$. From comparison of Figure 5 with the plot for A in Figure 3, we conclude that A is likely to anti-correlate with $S_{\rm ph}$ without a time lag.

In Figure 6, we show scatter plots of A, $\nu_{\rm max}$, and $\delta\nu_{\rm env}$ against $S_{\rm ph}$ from top to bottom, respectively, together with the best fits resulting from using 10 points and 9 points, as discussed above. When omitting the polluted data point, a pattern like that found in the Sun emerges: the envelope amplitudes (maximum frequency and envelope width) tend to anti-correlate (correlate) with magnetic activity. Nonetheless, the Pearson linear correlation coefficients and false alarm probabilities for $S_{\rm ph}$ vs. A, $S_{\rm ph}$ vs. $\nu_{\rm max}$, and $S_{\rm ph}$ vs. $\delta\nu_{\rm env}$ are $r = -0.4693$ with $P = 0.2025$, $r = 0.2320$ with $P = 0.5481$, and $r = 0.3334$ with $P = 0.3806$, respectively, indicating that the correlations are statistically insignificant. We suspect that the $S_{\rm ph}$ from the light curves of HD 49933 does not trace the magnetic activity level of HD 49933 closely enough. Therefore, it appears more secure and effective to associate the global asteroseismic parameters than to produce a photometric magnetic activity proxy to correlate the global asteroseismic parameters afterward.

4. HD 49933 IN SEISMIC H–R DIAGRAM

In Figure 7, we show the seismic Hertzsprung–Russell diagram showing the large separation, $\Delta\nu$, as a function of the effective temperature, $T_{\rm eff}$. Evolutionary

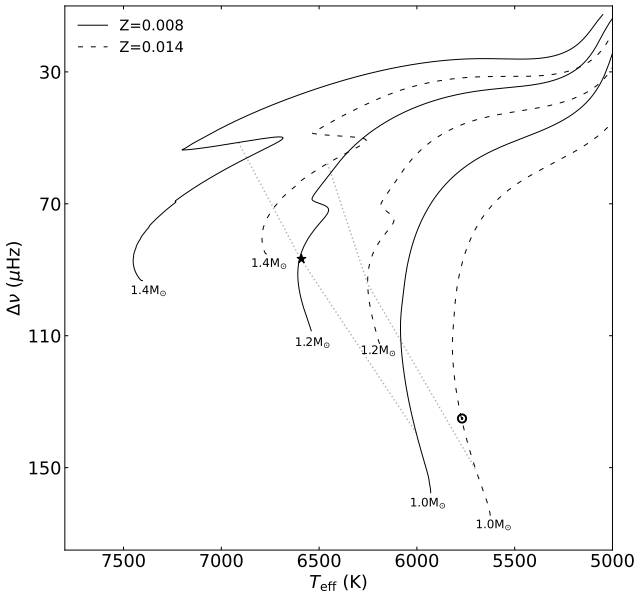

Figure 7. Seismic Hertzsprung–Russell diagram showing the large separation, $\Delta\nu$, as a function of the effective temperature, $T_{\rm eff}$, with evolutionary tracks. The dotted gray lines connect the positions where the star is ~ 2.25 Gyr old, respectively. The locations of HD 49933 and the Sun are marked with an asterisk and its common sign ($\odot$), respectively. The solid and dashed curves result from two chemical compositions of $Z = 0.008$ and $Z = 0.014$ for a given mass denoted in the bottom of individual curves, respectively.

tracks from main sequence to sub-giants, computed with the Modules for Experiments in Stellar Astrophysics (MESA) code (Paxton et al. 2019 and references therein), are shown for masses of $1.0M_\odot$, $1.2M_\odot$, and $1.4M_\odot$ from right to left. MESA is capable of not only including the physics governing the stellar evolution but also of coupling with two oscillations codes: ADIPLS (Christensen-Dalsgaard 2008) and the non-adiabatic code GYRE (Townsend & Teitler 2013). Nonetheless, we have not taken into account rotation and diffusion in these particular calculations. The solid and dashed curves result from two different metallicities of $Z = 0.008$ and $Z = 0.014$ for a given stellar mass, respectively. The corresponding $\Delta\nu$ in the model calculations is estimated using the scaling relation (Kjeldsen & Bedding 2011; Huber et al. 2011; Stello et al. 2011)

$$\Delta\nu = \left(\frac{M}{M_\odot}\right)^{1/2} \left(\frac{T_{\rm eff}}{T_{\rm eff,\odot}}\right)^{3} \left(\frac{L}{L_\odot}\right)^{3/4} \Delta\nu_\odot, \qquad (3)$$

where $\Delta\nu_\odot = 135.1$ μHz was derived from the analysis of level-2 data taken by the GREEN channel of the Variability of solar Irradiance and Gravity Oscillations/Sun PhotoMeters (VIRGO/SPM) (Kim & Chang 2021b). Errors in use of the scaling relation owing to $T_{\rm eff}$ and metallicity are known to be only about a few percent (White et al. 2011; Miglio et al. 2013; Mosser et al. 2013; Guggenberger et al. 2016; Sharma et al. 2016; Rodrigues et al. 2017; Ong & Basu 2019).

Now, to locate HD 49933 in the seismic H–R diagram, we have first determined $\Delta\nu$ by using a power spectrum method (Hekker et al. 2010; Mathur et al. 2010; Viani et al. 2019). The $\Delta\nu$ found from the power spectrum of entire time series for HD 49933 is 86.69 μHz, which is compatible with reported values (Appourchaux et al. 2008; Benomar et al. 2009). The stellar parameters of HD 49933 are summarized in Table 1. For the effective temperature of HD 49933 we have adopted the value of 6590 K from Bruntt (2009), which is derived from Strömgren photometry. We note that, depending on the spectroscopic and photometric methodology, values for the effective temperature range from 6450 K to 6780 K (Bruntt et al. 2004, 2008; Gillon & Magain 2006; Kallinger et al. 2010). The position of HD 49933 in the seismic H–R diagram suggests the mass of HD 49933 around $1.2M_\odot$ and a metallicity lower than that of the Sun; actually, mass estimates for HD 49933 span the range 1.08–1.34 $M_\odot$, depending on how physical effects such as rotation, microscopic diffusion, and overshooting of the convective core is dealt with (e.g., Liu et al. 2014). We note that, together with asteroseismic and non-asteroseismic data, the reported mass of HD 49933 seems to converge to a value slightly above $1.2M_\odot$ with $Z = 0.008$ in any case (Piau et al. 2009; Benomar et al. 2010; Kallinger et al. 2010; Bigot et al. 2011), which is close to our estimated value.

5. SUMMARY AND CONCLUSIONS

Thanks to long and accurate helioseismic observations, it has been known for more than 30 years that solar acoustic mode parameters change with the solar activity level. It is thus reasonable to expect that the observed parameters of the stellar acoustic mode also vary accordingly as the stellar magnetic cycle proceeds. However, it is necessary to make use of additional observables to ensure that the observed variability is indeed activity-induced, since not all observed variations may be consistent with an activity-related origin. Using ensemble asteroseismology, we statistically analyzed the photometric light curve of HD 49933 recorded by the CoRoT satellite, calculating the acoustic power spectrum with the Lomb-Scargle algorithm and then fitting a model to the observed power spectrum.

Our main findings are as follows:

(1) The amplitude of the envelope significantly anti-correlates with both the maximum frequency of the envelope profile and the width of the envelope unless superflare-like events strongly contaminate the light curves. We conclude that the global asteroseismic parameters can be utilized for cross-checking asteroseismic detections of activity-related variations in Sun-like stars.

(2) Even though the photometric proxy for stellar magnetic activity apparently shows the expected scalings with the global asteroseismic parameters, they are statistically insignificant. We suspect that it is more secure and effective to associate the global asteroseismic parameters than to produce a photometric magnetic activity proxy to indirectly correlate the global

asteroseismic parameters.

(3) Based on our determination of $\Delta\nu$ with evolutionary tracks computed by the MESA code, the mass of HD 49933 is found to be around 1.2 $M_{\odot}$ with a sub-solar metallicity of $Z = 0.008$, which agrees with the current consensus from with asteroseismic and non-asteroseismic data.

Unlike the observed parameters of the individual acoustic modes of Sun-like stars, which have been shown to follow trends similar to that observed in the Sun, the statistical behavior of the global asteroseismic parameters in magnetically active Sun-like stars is only partially understood. Here, we have probed whether the relations among the global seismic parameters can be utilized for cross-checking asteroseismic detections of activity-related variations in Sun-like stars. Indeed, we find that the envelope amplitude and activity of the Sun are negatively correlated and that the envelope width shows a correlation with the solar activity (Kim & Chang 2021b).

ACKNOWLEDGMENTS

The authors thank the anonymous referees for critical comments and helpful suggestions which greatly improved the original version of the manuscript. This study was funded by the Basic Science Research Program through the National Research Foundation (NRF) of Korea funded by the Ministry of Science, ICT and Future Planning (2018R1A6A1A06024970). HYC was supported by a National Research Foundation of Korea Grant funded by the Korean government (NRF-2018R1D1A3B070421880).

REFERENCES

Aerts, C., Christensen-Dalsgaard, J., & Kurtz, D. W. 2010, Asteroseismology, Astronomy and Astrophysics Library (Berlin: Springer)

Ak, T., Ozkan, M. T., & Mattei, J. A. 2001, Solar-type Cycles of the Secondary Stars in Cataclysmic Variables, A&A, 369, 882

Appourchaux, T., Michel, E., Auvergne, M., et al. 2008, CoRoT Sounds the Stars: p-mode Parameters of Sun-like Oscillations on HD 49933, A&A, 488, 705

Appourchaux, T., Belkacem, K., Broomhall, A.-M., et al. 2010, The Quest for the Solar g Modes, A&ARv, 18, 197

Arentoft, T., Kjeldsen, H., Bedding, T. R., et al. 2008, A Multisite Campaign to Measure Solar-like Oscillations in Procyon. I. Observations, Data Reduction, and Slow Variations, ApJ, 687, 1180

Baglin, A., Auvergne, M., Barge, P., et al. 2006, Scientific Objectives for a Minisat: CoRoT, The CoRoT Mission Pre-Launch Status – Stellar Seismology and Planet Finding, ESA Special Publication, 1306, 33

Baliunas, S. L., Donahue, R. A., Soon, W. H., et al. 1995, Chromospheric Variations in Main-Sequence Stars. II, ApJ, 438, 269

Balmforth, N. J. 1992, Solar Pulsational Stability – III. Acoustical Excitation by Turbulent Convection, MNRAS, 255, 639

Basu, S., Christensen-Dalsgaard, J., Chaplin, W. J., et al. 1997, Solar Internal Sound Speed as Inferred from Combined BiSON and LOWL Oscillation Frequencies, MNRAS, 292, 243

Bedding, T. R., Kjeldsen, H., Campante, T. L., et al. 2010, A Multi-Site Campaign to Measure Solar-Like Oscillations in Procyon. II. Mode Frequencies, ApJ, 713, 935

Belkacem, K., Goupil, M. J., Dupret, M. A., et al. 2011, The Underlying Physical Meaning of the $\nu_{\rm max}$–$\nu_{\rm c}$ Relation, A&A, 530, A142

Belkacem, K., Samadi, R., Mosser, B., et al. 2013, Progress in Physics of the Sun and Stars: A New Era in Helio- and Asteroseismology, ASPC, 479, 61

Benomar, O., Appourchaux, T., & Baudin, F. 2009, The Solar-like Oscillations of HD 49933: A Bayesian Approach, A&A, 506, 15

Benomar, O., Baudin, F., Marques, J. P., et al. 2010, Spectrum Analysis and Seismic Interpretation of a Solar-like Pulsator (HD 49933) Observed by CoRoT, AN, 331, 956

Bigot, L., Mourard, D., Berio, P., et al. 2011, The Diameter of the CoRoT Target HD 49933. Combining the 3D limb Darkening, Asteroseismology, and Interferometry, A&A, 534, L3

Böhm-Vitense, E. 2007, Chromospheric Activity in G and K Main-Sequence Stars, and What It Tells Us about Stellar Dynamos, ApJ, 657, 486

Brown, T. M., & Gilliland, R. L. 1994, Asteroseismology, ARA&A, 32, 37

Bruntt, H., Bikmaev, I. F., Catala, C., et al. 2004, Abundance Analysis of Targets for the COROT/MONS Asteroseismology Missions. II. Abundance Analysis of the COROT Main Targets, A&A, 425, 683

Bruntt, H., De Cat, P., & Aerts, C. 2008, A Spectroscopic Study of Southern (Candidate) γ Doradus Stars. II. Detailed Abundance Analysis and Fundamental Parameters, A&A, 478, 487

Bruntt, H. 2009, Accurate Fundamental Parameters of CoRoT Asteroseismic Targets. The Solar-like Stars HD 49933, HD 175726, HD 181420, and HD 181906, A&A, 506, 235

Cenarro, A. J., Peletier, R. F., Sánchez-Blázquez, P., et al., 2007, Medium-resolution Isaac Newton Telescope Library of Empirical Spectra – II. The Stellar Atmospheric Parameters, MNRAS, 374, 664

Chaintreuil, S., Deru, A., Baudin, F., et al. 2016, The "Ready to Use" CoRoT Data, The CoRoT Legacy Book: The Adventure of the Ultra High Precision Photometry from Space, 61 (Les Ulis: EDP Sciences)

Chaplin, W. J., Elsworth, Y., Isaak, G. R., et al. 1998, An Analysis of Solar p-mode Frequencies Extracted from BiSON Data: 1991–1996, MNRAS, 300, 1077

Chaplin, W. J., Elsworth, Y., Isaak, G. R., et al. 2000, Variations in the Excitation and Damping of Low-l Solar p Modes over the Solar Activity Cycle, MNRAS, 313, 32

Chaplin, W. J., Appourchaux, T., Elsworth, Y., et al. 2001, The Phenomenology of Solar-cycle-induced Acoustic Eigenfrequency Variations: A Comparative and Complementary Analysis of GONG, BiSON and VIRGO/LOI Data, MNRAS, 324, 910

Chaplin, W. J., Elsworth, Y., Isaak, G. R., et al. 2004, The Solar Cycle as Seen by Low-l p-mode Frequencies: Comparison with Global and Decomposed Activity Proxies, MNRAS, 352, 1102

Chaplin, W. J., Elsworth, Y., Houdek, G., et al. 2007, On Prospects for Sounding Activity Cycles of Sun-like Stars with Acoustic Modes, MNRAS, 377, 17

Chaplin, W. J., Bedding, T. R., Bonanno, A., et al. 2011, Evidence for the Impact of Stellar Activity on the De-

tectability of Solar-like Oscillations Observed by Kepler, ApJL, 732, L5
Chaplin, W. J., & Miglio, A. 2013, Asteroseismology of Solar-Type and Red-Giant Stars, ARA&A, 51, 353
Christensen-Dalsgaard, J., Duvall, T. L., Gough, D. O., et al. 1985, Speed of Sound in the Solar Interior, Nature, 315, 378
Christensen-Dalsgaard, J. 1988, A Hertzsprung-Russell Diagram for Stellar Oscillations, Advances in Helio- and Asteroseismology, Proc. IAU, 123, 295
Christensen-Dalsgaard, J. 2002, Helioseismology, RvMP, 74, 1073
Christensen-Dalsgaard, J. 2008, ADIPLS – The Aarhus Adiabatic Oscillation Package, Ap&SS, 316, 113
Dall, T. H., Bruntt, H., Stello, D., et al. 2010, Solar-like Oscillations and Magnetic Activity of the Slow Rotator EK Eridani, A&A, 514, A25
Elsworth, Y., Howe, R., Isaak, G. R., et al. 1990, Variation of Low-order Acoustic Solar Oscillations over the Solar Cycle, Nature, 345, 322
Elsworth, Y., Howe, R., Isaak, G. R., et al. 1993, The Variation in the Strength of Low-l Solar p-modes – 1981–92, MNRAS, 265, 888
Elsworth, Y., Howe, R., Isaak, G. R., et al. 1994, Solar p-Mode Frequencies and Their Dependence on Solar Activity: Recent Results from the BISON Network, ApJ, 434, 801
Elsworth, Y., Howe, R., Isaak, G. R., et al. 1995, Slow Rotation of the Sun's Interior, Nature, 376, 669
Fossat, E., Gelly, B., Grec, G., et al. 1987, Search for Solar P-Mode Frequency Changes Between 1980 and 1985, A&A, 177, L47
Pallé, P. L., Regulo, C., & Roca Cortes, T. 1989, Solar Cycle Induced Variations of the Low L Solar Acoustic Spectrum, A&A, 224, 253
Goldreich, P., & Keeley, D. A. 1977, Solar Seismology. II. The Stochastic Excitation of the Solar p-modes by Turbulent Convection, ApJ, 212, 243
Goldreich, P., & Kumar, P. 1988, The Interaction of Acoustic Radiation with Turbulence, ApJ, 326, 462
Goldreich, P., Murray, N., & Kumar, P. 1994, Excitation of Solar p-Modes, ApJ, 424, 466
Gontcharov, G. A., 2006, Pulkovo Compilation of Radial Velocities for 35 495 Hipparcos Stars in a Common System, AstL, 32, 759
Gough, D. 1985, Inverting Helioseismic Data, Sol. Phys., 100, 65
Gough, D. O. 1990, Comments on Helioseismic Inference, Progress of Seismology of the Sun and Stars, LNP, 367, 283
García, R. A., Mathur, S., Salabert, D., et al. 2010, CoRoT Reveals a Magnetic Activity Cycle in a Sun-Like Star, Science, 329, 1032
Gelly, B., Lazrek, M., Grec, G., et al. 2002, Solar p-modes from 1979 Days of the GOLF Experiment, A&A, 394, 285
Gillon, M., & Magain, P. 2006, High Precision Determination of the Atmospheric Parameters and Abundances of the COROT Main Targets, A&A, 448, 341
Guggenberger, E., Hekker, S., Basu, S., et al. 2016, Significantly Improving Stellar Mass and Radius Estimates: A New Reference Function for the $\Delta\nu$ Scaling Relation, MNRAS, 460, 4277
Hekker, S., Broomhall, A.-M., Chaplin, W. J., et al. 2010, The Octave (Birmingham-Sheffield Hallam) Automated Pipeline for Extracting Oscillation Parameters of Solar-like Main-sequence Stars, MNRAS, 402, 2049
Hekker, S. 2020, Scaling Relations for Solar-like Oscillations: A Review, Front. Astron. Space Sci., 7, 3
Henry, T. J., Soderblom, D. R., Donahue, R. A., et al. 1996, A Survey of Ca II H and K Chromospheric Emission in Southern Solar-Type Stars, AJ, 111, 439
Howe, R., Komm, R. W., & Hill, F. 2002, Localizing the Solar Cycle Frequency Shifts in Global p-Modes, ApJ, 580, 1172
Howe, R., Chaplin, W. J., Basu, S., et al. 2020, Solar Cycle Variation of $\nu_{\rm max}$ in Helioseismic Data and Its Implications for Asteroseismology, MNRAS, 493, L49
Huber, D., Bedding, T. R., Stello, D., et al. 2011, Testing Scaling Relations for Solar-like Oscillations from the Main Sequence to Red Giants Using Kepler Data, ApJ, 743, 143
Isaacson, H., & Fischer, D. 2010, Chromospheric Activity and Jitter Measurements for 2630 Stars on the California Planet Search, ApJ, 725, 875
Jiménez, A., García, R. A., & Pallé, P. L. 2011, The Acoustic Cutoff Frequency of the Sun and the Solar Magnetic Activity Cycle, ApJ, 743, 99
Jiménez-Reyes, S. J., García, R. A., Jiménez, A., et al. 2003, Excitation and Damping of Low-Degree Solar p-Modes during Activity Cycle 23: Analysis of GOLF and VIRGO Sun Photometer Data, ApJ, 595, 446
Jo, Y. A., Kim, K., & Chang, H. Y. 2021, in preparation
Kallinger, T., Gruberbauer, M., Guenther, D. B., et al. 2010, The Nature of p-modes and Granulation in HD 49933 Observed by CoRoT, A&A, 510, A106
Karoff, C. 2008, Observational Asteroseismology, Ph.D. Thesis, Aarhus University
Kim, K., & Chang, H. Y. 2021a, Scaling Relations for Width of the Power Excess of Stellar Oscillations, New Astron., 84, 101522
Kim, K., & Chang, H. Y. 2021b, Do the Observed Relations of the Global Seismic Parameters on the Magnetic Activity Level?, JKAS, 54, 121
Kjeldsen, H. & Bedding, T. R. 1995, Amplitudes of Stellar Oscillations: The Implications for Asteroseismology, A&A, 293, 87
Kjeldsen, H., Bedding, T. R., Arentoft, T., et al. 2008, The Amplitude of Solar Oscillations Using Stellar Techniques, ApJ, 682, 1370
Kjeldsen, H., & Bedding, T. R. 2011, Amplitudes of Solar-like oscillations: A New Scaling Relation, A&A, 529, L8
Komm, R. W., Howe, R., & Hill, F. 2000, Solar-Cycle Changes in Gong P-Mode Widths and Amplitudes 1995–1998, ApJ, 531, 1094
Libbrecht, K. G., & Woodard, M. F. 1990, Solar-cycle Effects on Solar Oscillation Frequencies, Nature, 345, 779
Liu, Z., Yang, W., Bi, S., et al. 2014, Asteroseismic Analysis of the CoRoT Target HD 49933, ApJ, 780, 152
Lomb, N. R. 1976, Least-Squares Frequency Analysis of Unequally Spaced Data, Ap&SS, 39, 447
Mathur, S., García, R. A., Régulo, C., et al. 2010, Determining Global Parameters of the Oscillations of Solar-like Stars, A&A, 511, A46
Mathur, S., García, R. A., Ballot, J., et al. 2014, Magnetic Activity of F Stars Observed by Kepler, A&A, 562, A124
Metcalfe, T. S., Dziembowski, W. A., Judge, P. G., et al. 2007, Asteroseismic Signatures of Stellar Magnetic Activity Cycles, MNRAS, 379, L16
Meunier, N., Lagrange, A.-M., & Cuzacq, S. 2019, Activity Time Series of Old Stars from Late F to Early K. IV.

Limits of the Correction of Radial Velocities Using Chromospheric Emission, A&A, 632, A81
Michel, E., Baglin, A., Weiss, W. W., et al. 2008, First Asteroseismic Results from CoRoT, Commun. Asteroseismol. 156, 73
Miglio, A., Chiappini, C., Morel, T., et al. 2013, Galactic Archaeology: Mapping and Dating Stellar Populations with Asteroseismology of Red-giant Stars, MNRAS, 429, 423
Mosser, B., Bouchy, F., Catala, C., et al. 2005, Seismology and Activity of the F Type Star HD 49933, A&A, 431, L13
Mosser, B., Baudin, F., Lanza, A. F., et al. 2009, Short-lived Spots in Solar-like Stars as Observed by CoRoT, A&A, 506, 245
Mosser, B., Michel, E., Belkacem, K., et al. 2013, Asymptotic and Measured Large Frequency Separations, A&A, 550, A126
Ong, J. M. J., & Basu, S. 2019, Explaining Deviations from the Scaling Relationship of the Large Frequency Separation, ApJ, 870, 41
Paxton, B., Smolec, R., Schwab, J., et al. 2019, Modules for Experiments in Stellar Astrophysics (MESA): Pulsating Variable Stars, Rotation, Convective Boundaries, and Energy Conservation, ApJS, 243, 10
Piau, L., Turck-Chièze, S., Duez, V., et al. 2009, Impact of the Physical Processes in the Modeling of HD 49933, A&A, 506, 175
Pires, S., Mathur, S., García, R. A., et al. 2015, Gap Interpolation by Inpainting Methods: Application to Ground and Space-based Asteroseismic Data, A&A, 574, A18
Radick, R. R., Lockwood, G. W., Skiff, B. A., et al. 1998, Patterns of Variation among Sun-like Stars, ApJS, 118, 239
Régulo, C., García, R. A., & Ballot, J. 2016, Magnetic Activity Cycles in Solar-like Stars: The Cross-correlation Technique of p-mode Frequency Shifts, A&A, 589, A103
Rodrigues, T. S., Bossini, D., Miglio, A., et al. 2017, Determining Stellar Parameters of Asteroseismic Targets: Going beyond the Use of Scaling Relations, MNRAS, 467, 1433
Saar, S. H., & Brandenburg, A. 1999, Time Evolution of the Magnetic Activity Cycle Period. II. Results for an Expanded Stellar Sample, ApJ, 524, 295
Salabert, D., Jiménez-Reyes, S. J., & Tomczyk, S. 2003, Study of p-mode Excitation and Damping Rate Variations from IRIS^{++} Observations, A&A, 408, 729
Salabert, D., Régulo, C., Ballot, J., et al. 2011, About the p-mode Frequency Shifts in HD 49933, A&A, 530, A127
Santos, Â. R. G., Campante, T. L., Chaplin, W. J., et al. 2018, Signatures of Magnetic Activity in the Seismic Data of Solar-type Stars Observed by Kepler, ApJS, 237, 17
Santos, Â. R. G., Campante, T. L., Chaplin, W. J., et al. 2019, Signatures of Magnetic Activity: On the Relation between Stellar Properties and p-mode Frequency Variations, ApJ, 883, 65
Scargle, J. D. 1982, Studies in Astronomical Time Series Analysis. II. Statistical Aspects of Spectral Analysis of Unevenly Spaced Data, ApJ, 263, 835
Sharma, S., Stello, D., Bland-Hawthorn, J., et al. 2016, Stellar Population Synthesis Based Modeling of the Milky Way Using Asteroseismology of 13,000 Kepler Red Giants, ApJ, 822, 15
Stello, D., Huber, D., Kallinger, T., et al. 2011, Amplitudes of Solar-like Oscillations: Constraints from Red Giants in Open Clusters Observed by Kepler, ApJL, 737, L10
Tassoul, M. 1980, Asymptotic Approximations for Stellar Nonradial Pulsations, ApJS, 43, 469
Thomas, A. E. L., Chaplin, W. J., Basu, S., et al. 2021, Impact of Magnetic Activity on Inferred Stellar Properties of Main-sequence Sun-like Stars, MNRAS, 502, 5808
Thompson, M. J., Toomre, J., Anderson, E. R., et al. 1996, Differential Rotation and Dynamics of the Solar Interior, Science, 272, 1300
Townsend, R. H. D., & Teitler, S. A. 2013, GYRE: An Open-source Stellar Oscillation Code based on a New Magnus Multiple Shooting Scheme, MNRAS, 435, 3406
Ulrich, R. K. 1986, Determination of Stellar Ages from Asteroseismology, ApJL, 306, L37
van Leeuwen, F., 2007, Validation of the New Hipparcos Reduction, A&A, 474, 653
Viani, L. S., Basu, S., Corsaro, E., et al. 2019, Determining the Best Method of Calculating the Large Frequency Separation For Stellar Models, ApJ, 879, 33
White, T. R., Bedding, T. R., Stello, D., et al. 2011, Calculating Asteroseismic Diagrams for Solar-like Oscillations, ApJ, 743, 161
Woodard, M. F., & Noyes, R. W. 1985, Change of Solar Oscillation Eigenfrequencies with the Solar Cycle, Nature, 318, 449